



Decreasing diversity of rare bacterial subcommunities relates to dissolved organic matter along permafrost thawing gradients



Lei Zhou^{a,b}, Yongqiang Zhou^{a,b}, Xiaolong Yao^{a,b}, Jian Cai^{a,b}, Xin Liu^c, Xiangming Tang^{a,b}, Yunlin Zhang^{a,b,*}, Kyoung-Soon Jang^d, Erik Jeppesen^{e,f,g}

^a Taihu Laboratory for Lake Ecosystem Research, State Key Laboratory of Lake Science and Environment, Nanjing Institute of Geography and Limnology, Chinese Academy of Sciences, Nanjing 210008, China

^b University of Chinese Academy of Sciences, Beijing 100049, China

^c Shanghai Municipal Engineering Design Institute (Group) CO., LTD, Shanghai 200092, China

^d Biomedical Omics Group, Korea Basic Science Institute, Cheongju 28119, South Korea

^e Department of Bioscience and Arctic Research Centre, Aarhus University, DK-8600 Silkeborg, Denmark

^f Sino-Danish Centre for Education and Research, Beijing 100190, China

^g Limnology Laboratory and EKOSAM, Department of Biological Sciences, Middle East Technical University, Ankara, Turkey

ARTICLE INFO

Keywords:

Permafrost thawing
Bacterial diversity
Co-occurrence networks
Microbial metabolism
Dissolved organic matter
Ultrahigh-resolution mass spectrometry

ABSTRACT

Dissolved organic matter (DOM) released from permafrost thaw greatly influences the biogeochemical cycles of, among others, downstream carbon, nitrogen and phosphorus cycles; yet, knowledge of the linkages between bacterial communities with permafrost DOM heterogeneity is limited. Here, we aim at unravelling the responses of bacterial diversities and metabolic profiles to DOM quantity and composition across permafrost thawing gradients by coupling an extensive field investigation with bio-incubation experiments. Richness, evenness and dissimilarities of the whole and rare communities decreased from thermokarst pits to headstreams and to downstream rivers. The assemblages of the abundant subcommunities were mainly determined by ecological drift-driven stochastic processes. Both the optical and the molecular composition of DOM were significantly related to the changes of the whole (rare) bacterial communities (Mantel's correlation > 0.5, $p < 0.01$). Diversity indices of the whole and rare communities decreased with decreasing relative abundance of tannins, condensed aromatics and more aromatic and oxidized lignins as well as with decreased dissolved organic carbon and intensities of all fluorescence components. Laboratory DOM bio-incubation experiments further confirmed microbial consumption of more aromatic and oxidized compounds as well as decreasing metabolic diversities in terms of microbial degradation and production along permafrost thawing gradients. Our findings suggest that changes in the sources of permafrost-derived DOM induced by global warming can have different influences on the diversity and metabolism of bacterial communities and thus on permafrost carbon climate feedbacks along permafrost thawing gradients.

1. Introduction

Permafrost contains approximately 50% of the global soil carbon (McCalley et al., 2014). As ice-rich permafrost thaws, topographic depressions (thermokarsts) can act as a source of dissolved organic matter (DOM) and thus contribute to the biogeochemical cycles of, among others, downstream carbon, nitrogen and phosphorus (Kothawala et al., 2014; Spencer et al., 2008; Ward et al., 2017). DOM can be mineralised by microbes and release greenhouse gas (Drake et al., 2015; Schuur et al., 2009), resulting in a positive feedback to climate warming, which

differs in extent across thawing gradients from thermokarsts to downstream aquatic ecosystems (Chen et al., 2019; Cory et al., 2013; Kramshoj et al., 2019; Schuur et al., 2015). Thus, understanding the microbial responses to permafrost-derived DOM is vital for determining its effects on the global carbon cycling.

Permafrost-derived DOM undergoes a series of transformations including leaching, mineralisation and photochemical alteration once released from the soils, leading to various chemical and biodegradable changes of DOM across permafrost thawing gradients (Chen et al., 2018; Crevecoeur et al., 2015; Roehm et al., 2009; Ward and Cory,

* Corresponding author at: Yunlin Zhang, Nanjing Institute of Geography and Limnology, Chinese Academy of Sciences, 73 East Beijing Road, Nanjing 210008, China.

E-mail address: ylzhang@niglas.ac.cn (Y. Zhang).

2015). Photochemical alteration of dissolved organic carbon (DOC) draining permafrost soils shifts microbial metabolic pathways and stimulates respiration (Ward et al., 2017). In addition, permafrost DOM optical properties are correlated with bacterial growth and community composition in permafrost-linked freshwaters and ponds (Roiha et al., 2016; Watanabe et al., 2011). These results demonstrate that the variations in permafrost DOM quantity and composition play an important role for the diversity, composition and functioning of bacterial communities.

Bacterial communities normally comprise a few abundant and many rare species (Logares et al., 2014), and abundant and rare sub-communities may show fundamentally distinct characteristics and have different ecological roles (Pedros-Alio, 2012). Biodiversity is an important issue in community ecology, underpinning ecosystem functioning (Ren et al., 2017; Wilhelm et al., 2013; Zhang et al., 2019). Characterising species diversity and its variation along environmental gradients and understanding the forces that structure bacterial communities are fundamental components of ecological research (Anderson et al., 2011; Cottenie, 2005; Dumbrell et al., 2010). Previous studies have mainly focused on abundant species and emphasised their contribution to the total biomass as well as the carbon and nutrient cycling (Pedros-Alio, 2012). Owing to high-throughput sequencing technologies, rare taxa are increasingly recognised as drivers of key functions in terrestrial and aquatic ecosystems, and their ecological role may be more important than that of abundant bacteria (Campbell et al., 2011; Jousset et al., 2017; Lynch and Neufeld, 2015). However, the linkages between biodiversity patterns of abundant and rare bacterial sub-communities with the change of permafrost DOM across permafrost thawing gradients have not been explored.

The Qinghai-Tibetan Plateau, accounting for approximately 70% of the global alpine permafrost (Bockheim and Munroe, 2014), is widespread with thermokarst initiation due to climate warming (Mu et al., 2016). These thermo-erosion pits or gullies lead to the transfer of a large amount of DOM to nearby streams (Wang et al., 2018a). In-depth and high-resolution characterisation of both diverse bacterial communities and complex DOM compounds is, however, a prerequisite to link DOM composition with bacterial communities (Logue et al., 2016). We applied Fourier transform ion cyclotron resonance mass spectrometry (FT-ICR MS), a highly powerful ultrahigh-resolution method for obtaining detailed information on DOM elemental composition, together with optical measurements to characterise DOM quantity and quality. High-throughput sequencing was conducted for bacterial community analysis to unveil the responses of both abundant and rare sub-communities to the change of DOM in this region. To further elucidate the metabolic functions of the microbial community in regard to the consumption and production of DOM, we conducted DOM bio-incubation experiments to examine changes of DOM composition after microbial processing.

The aims of our study were to (i) explore the biodiversity patterns of abundant and rare taxa across permafrost thawing gradients; (ii) examine how bacterial assemblages and metabolic profiles respond to the quantity and composition of permafrost DOM, even at the molecular level. This study may improve our understanding of the linkages between microbes and DOM, which play a central role in biogeochemical cycles (Heimann and Reichstein, 2008; Ruiz-Gonzalez et al., 2015).

2. Materials and methods

2.1. Study sites and sample collection

Our study sites are located in Qilian County in the northern Qinghai-Tibetan Plateau. The continuous system where we conducted our sampling includes thermokarst-erosion pits of organic layer over headstreams to downstream rivers and thus covers evident permafrost thawing gradients with gradually decreasing DOC concentrations (Table S1). Sampling was carried out in May, July and September 2017.

Each month samples were randomly collected from thermokarst pits and headstreams and included 3 sites \times 3 replicates (Table S1). From rivers, the samples were taken in May, July and September and included 14 sites \times 3 replicates, 12 sites \times 3 replicates and 10 sites \times 3 replicates, respectively (Table S1). At each location, three replicates were taken within a 2–3 m radius to provide a representative sample. In addition, six spring, interflow and active layer samples were collected to allow comparisons with the samples from the pits, headstreams and rivers (Table S1). All samples were taken using acid-cleaned brown glass bottles and were kept dark and cold while in the field, after which they were immediately filtered (< 6 h) in the laboratory. Filtrates for physicochemical parameters and DOM measurements and filters for DNA extraction were stored at -20°C until further processing.

2.2. DOM bio-incubation experiments

Pit, headstream and river samples collected in July were incubated in the laboratory. Filtrates (100 mL) obtained after passing pre-rinsed 0.22 μm Millipore filters (47 mm diameter) to exclude particulate organic matter and bacteria were amended with 2 mL (2% of the unfiltered water) of the corresponding original samples as bacterial inoculum. To all incubation mixtures, we added nutrients consisting of 80 μM NH_4^+ and 10 μM PO_4^{3-} to avoid nutrient limitation. The samples were then incubated at room temperature ($20 \pm 2^{\circ}\text{C}$) for 28 days in the dark to facilitate comparisons with other bio-incubation studies (Abbott et al., 2014; Vonk et al., 2015). To ensure an adequate oxygen supply, pre-combusted (550°C for 6 h) and pre-rinsed brown incubation glass bottles were loosely capped and shaken daily.

2.3. Physicochemical parameters, fluorescence DOM measurements and parallel factor analysis (PARAFAC)

The elevation of each site was measured in the field. Water was collected and analysed for physicochemical parameters including total dissolved solids (TDS), pH, dissolved organic carbon (DOC), total dissolved nitrogen (TDN), total dissolved phosphorus (TDP), phosphate (PO_4^{3-}), nitrate (NO_3^-), nitrite (NO_2^-) and ammonium (NH_4^+). The samples were first filtered through pre-combusted (450°C for 4 h) Whatman GF/F filters of 0.7 μm porosity (for nutrients and DOC measurement) and subsequently through pre-rinsed 0.22 μm Millipore filters (for fluorescence DOM measurement) at low pressure to acid-cleaned brown glass bottles. Details on physicochemical parameters, fluorescence DOM measurements and parallel factor analysis (PARAFAC) are given in the Supplementary Material.

2.4. FT-ICR MS measurement

A total of 14 DOM samples, including 4 pit samples, 3 headstream samples and 7 river samples, were solid-phase extracted with PPL Bond Elut (Agilent) resins and then measured in negative mode electrospray ionization using a 15T FT-ICR mass spectrometer (solariXTM system, Bruker Daltonics, Billerica, MA) at the Korea Basic Science Institute, Ochang, Korea. Details on FT-ICR MS pre-treatment and measurement can be found in the Supplementary Material. van Krevelen diagrams were used to classify the assigned molecular formulae into seven categories (Ohno et al., 2014): (1) lipids ($\text{O/C} = 0\text{--}0.3$, $\text{H/C} = 1.5\text{--}2.0$), (2) proteins and amino sugars ($\text{O/C} = 0.3\text{--}0.67$, $\text{H/C} = 1.5\text{--}2.2$), (3) carbohydrates ($\text{O/C} = 0.67\text{--}1.2$; $\text{H/C} = 1.5\text{--}2$), (4) unsaturated hydrocarbons (UH, $\text{O/C} = 0\text{--}0.1$, $\text{H/C} = 0.7\text{--}1.5$), (5) lignins ($\text{O/C} = 0.1\text{--}0.67$, $\text{H/C} = 0.7\text{--}1.5$), (6) tannins ($\text{O/C} = 0.67\text{--}1.2$, $\text{H/C} = 0.5\text{--}1.5$), and (7) condensed aromatics ($\text{O/C} = 0\text{--}0.67$, $\text{H/C} = 0.2\text{--}0.7$).

2.5. DNA extraction, PCR, 16S rRNA gene sequencing and sequences processing

All 60 samples including 54 pit, headstream and river samples and 6 spring, interflow and active layer samples were filtered through 0.22 µm Millipore membranes (47 mm diameter) for bacterial community analysis. Details on DNA extraction, PCR, 16S rRNA gene sequencing and sequence processing are given in the [Supplementary Material](#). Operational taxonomic units (OTUs) were identified by clustering sequences with a 97% similarity threshold ([Edgar, 2010](#)). All archaea, eukaryotes, unclassified sequences and singletons (OTUs with only one sequence) were discarded from the whole dataset, and the subsample dataset was constructed according to the smallest sequencing effort.

2.6. Classification and functional annotation of abundant and rare taxa

Abundant and rare taxa were classified according to recent studies ([Xue et al., 2018](#)): abundant taxa (AT) are those with a relative abundance $\geq 0.01\%$ in all samples and $\geq 1\%$ in at least one sample; rare taxa (RT) are those with a relative abundance $< 0.01\%$ in at least one sample but never $\geq 1\%$ in any sample; moderate taxa (MT) with a relative abundance ranging from 0.01% to 1% in all samples; conditionally abundant and rare taxa (CART) with a relative abundance ranging from rare ($< 0.01\%$) to abundant ($\geq 1\%$). Numbers and portions of classified abundant and rare taxa are presented in [Table S2](#).

The functional annotation of prokaryotic taxa (FAPROTAX) was utilised to annotate taxa function associated with biogeochemistry processes. FAPROTAX identifies known taxa by employing marker gene sequencing and then estimates their metabolic phenotype based on experimental literature ([Louca et al., 2017](#)).

2.7. Diversity estimation and null model analysis

We calculated alpha-diversity using four indices including Chao1 (a nonparametric species richness estimator), Pielou's evenness, the Shannon index (a combination of richness and evenness) and Invsimpson (the inverse Simpson index). Beta-diversity (a measure of compositional differences among sites) was examined using two dissimilarity metrics: incidence-based Jaccard and abundance-based Bray-Curtis dissimilarity. Abundance-based Bray-Curtis dissimilarity can be separated into two components: (i) balanced changes in abundance, whereby the individuals of some species at one site are substituted by an equal number of individuals of different species at another site; (ii) abundance gradients, whereby some individuals are lost from one site to the other ([Baselga, 2013](#)).

To investigate the mechanism (i.e. deterministic or stochastic process) underlying the community assembly, we performed the null model analysis using abundance-based similarity metrics following previous studies ([Kraft et al., 2011](#); [Zhang et al., 2019](#); [Zhou et al., 2014](#)). If community assembly is primarily driven by deterministic processes, the real bacterial communities will be significantly different from corresponding null expectations as determined by the permutational analysis of multivariate dispersions (PERMDISP) test. In contrast, a stochastic process shapes the community assembly when the real bacterial community is not distinguishable from the null expectation. In addition, the standardised effect size (SES) was calculated as the differences in beta diversity between the real communities and the mean value of null communities divided by the standardised deviation of the beta diversity in the null communities. The relative importance of stochastic processes increases when SES is closer to zero.

2.8. Indicator OTUs and network analysis

We identified indicator OTUs in the pits, headstreams and rivers by using the "indicspecies" R package. This method calculates indicator

values for species across site groups and performs permutation tests to assess the statistical significance of species-site group associations ([Gáceres and Legendre, 2009](#)). We determined indicator OTUs across permafrost thawing gradients based on an association value > 0.6 and p -value < 0.05 assessed by 999 permutation tests.

To visualise OTUs co-occurrence network and the associations between OTUs and DOM formulae, networks were constructed by calculating pairwise Spearman rank correlation coefficients (r). For the OTUs co-occurrence network, OTUs with occurrence in more than 20% of all samples were selected to simplify the dataset. Valid co-occurrences with $r > 0.6$ or $r < -0.6$ and p -value < 0.05 were incorporated into networks. Considering the large dataset of molecular peaks, strong correlations with $r > 0.8$ or $r < -0.8$ and p -value < 0.01 between OTUs and assigned DOM formulae containing CHO, CHON, CHOS and CHONS were selected to construct the network. To reduce the chances of obtaining false-positive results, the p -values were adjusted with a multiple testing correction by the Benjamini-Hochberg method ([Benjamini and Hochberg, 1995](#)). Random networks with equal numbers of nodes and edges of the real networks were generated based on the Erdős-Rényi random networks ([Erdős and Rényi, 1960](#)). Network analyses were performed using the "igraph", "vegan" and "psych" packages in the R software. Network visualisation and module detection were conducted using the interactive platform Gephi (WebAtlas, Paris, France).

2.9. Statistical analyses

Non-metric multidimensional scaling (NMDS), coupled with analysis of similarity (ANOSIM), was used to visualise the compositional difference among site groups and to perform significance test of differences. The ANOSIM test statistics, R (ranges between 0 and 1), show the degree of separation among groups, with a score of 1 indicating complete separation and 0 no separation ([Clarke, 1993](#)). Other statistical analyses, including Mantel tests, Spearman's correlations, two-way analysis of variance (two-way ANOVA), nonparametric Wilcoxon test and Kruskal-Wallis rank test, multiple regression model analyses were performed using R software. Results of significance test with $p < 0.05$ were reported as significant.

2.10. Accession numbers

Sequence data were deposited at the National Center for Biotechnology Information under accession number PRJNA564189.

3. Results

3.1. Alpha-diversity and bacterial composition across permafrost thawing gradients

A total of 843,463 high-quality sequences and 11,871 OTUs were identified across all the samples. 19 OTUs (0.16%) containing 21.76% of all sequences were abundant and persistent in all samples; 11,687 OTUs (98.55%) containing 60.14% of all sequences were classified into rare taxa. The others (165 OTUs) were all affiliated to conditionally abundant and rare taxa ([Table S2](#)).

Alpha-diversity indices of all and rare taxa, including Chao1, Shannon, Invsimpson and Pielou's evenness, displayed similar patterns, and all indices differed significantly between sites rather than between months (two-way ANOVA, $p < 0.05$; [Table S3](#)). The difference was mainly caused by the river samples ([Fig. S1](#)), which showed significantly lower richness and evenness than the pit and headstream samples for the whole and rare communities (Wilcoxon test, $p < 0.05$), whereas no significant difference emerged between the pit and headstream samples ([Fig. S1](#)). In contrast, abundant taxa did not differ significantly between sites or month (two-way ANOVA, $p > 0.05$; [Table S3](#)) but had a relatively high F-value under the interaction effect

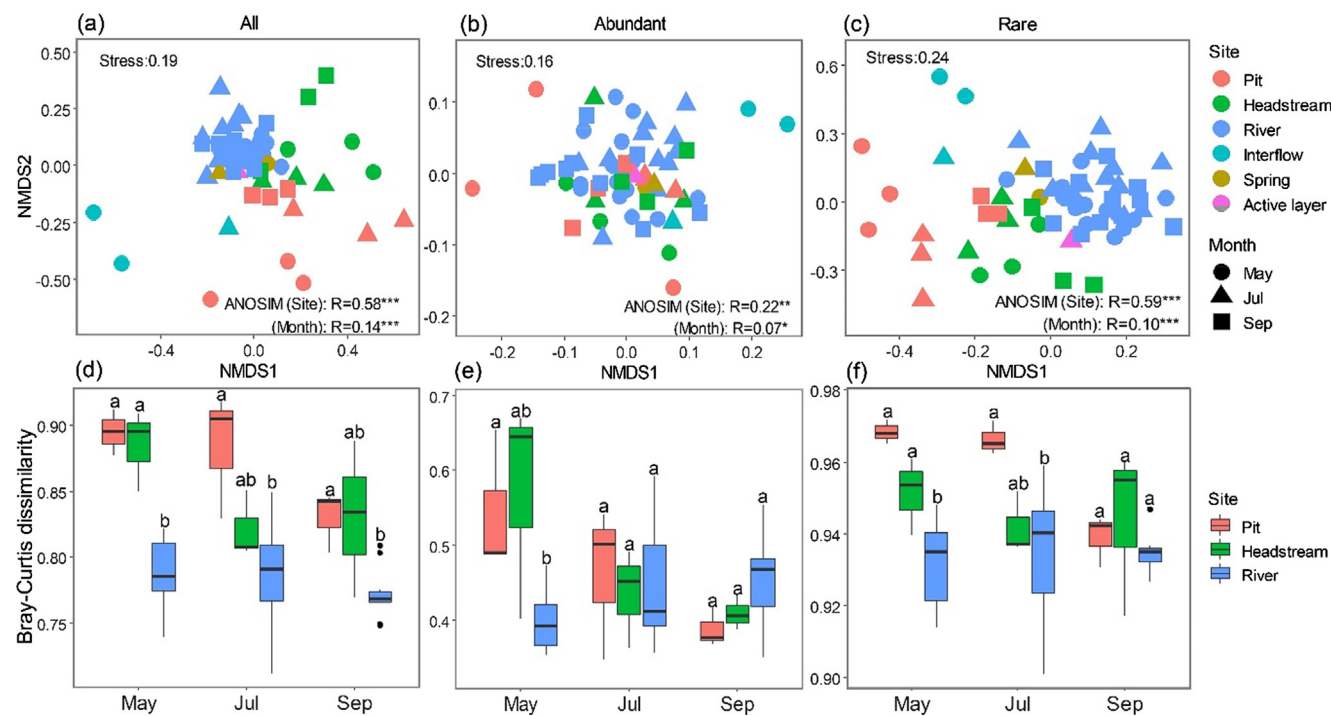


Fig. 1. Non-metric multidimensional scaling (NMDS) based on Bray-Curtis dissimilarity for the whole, abundant and rare communities (a–c). Comparisons of Bray-Curtis dissimilarities of the pit, headstream and river samples in different months for the whole, abundant and rare communities (d–f). Significant ($p < 0.05$) differences among the different sites are indicated by letters above the boxes. Boxes with same letters indicate (e.g. a, ab) no significant difference among groups determined by nonparametric Wilcoxon test, boxes with different letters (e.g. a, b) indicate significant differences among groups.

of site and month (Table S3).

Different sites showed distinct bacterial compositions (Fig. S2). Among the abundant phyla and classes (average relative abundance $> 1\%$), the relative abundances of *Firmicutes*, *Bacteroidetes* and *Betaproteobacteria* gradually increased from pits to headstreams and to rivers, whereas *Parcubacteria* gradually decreased. 78.9% of the abundant OTUs (15 OTUs) belonged to the abundant genus *Exiguobacterium* (Fig. S2), which is reported to survive at varying temperature extremes and to tolerate high levels of UV radiation (Ordoñez et al., 2013; Singh et al., 2013). Additionally, all indicator OTUs in pits, headstreams and rivers were composed of rare taxa and conditionally abundant and rare taxa (Table S4).

3.2. Bacterial beta-diversity and null model analyses

NMDS based on Bray-Curtis dissimilarity displayed the differences in bacterial communities among sites and months in the permafrost thawing environment (Fig. 1). Both the whole and the rare communities clustered more strongly by site than by month (Fig. 1), which is supported by the much higher R value determined by ANOSIM when the samples were grouped by site ($R > 0.58$) than by month ($R < 0.14$; Fig. 1). NMDS based on Jaccard dissimilarities showed similar patterns (Fig. S3). In contrast, the abundant subcommunities showed a much lower cluster effect by site (ANOSIM $R = 0.22$; Fig. 1) than the rare subcommunities. The clustering effect by site of the conditionally abundant and rare subcommunities was higher than that of the abundant subcommunities but lower than that of the rare subcommunities (Fig. S3). However, both month and site were significant factors in shaping bacterial communities (ANOSIM $p < 0.05$; Fig. 1; Fig. S3). The Bray-Curtis dissimilarity of rare taxa (0.96 ± 0.01) was significantly higher than that of abundant taxa (0.46 ± 0.10 , Wilcoxon test, $p < 0.05$; Fig. 1; Table S5).

Beta-diversity partitioning analysis was performed for pit, headstream and river samples, respectively. All results indicated that almost all of the Bray-Curtis dissimilarities of the whole and the rare

communities ($> 99\%$) derived from balanced variation in abundances between sites (i.e. replacement), whereas the dissimilarity of the abundant subcommunities mainly ($> 75\%$) was caused by unidirectional abundance gradients (i.e. species nestedness; Table S5). Two types of null model analyses were conducted. PERMDISP test revealed that the whole and the rare communities differed significantly from the null expectation (only stochastic community assembly processes included) regardless of sampling types ($p < 0.01$), indicating the dominant position of deterministic community assembly for the whole and the rare communities (Table S6). However, the observed abundant communities were not notably different from the null expectation, indicating that the stochasticity of the community assembly was more important than the determinism for the abundant communities (Table S6). The value of SES, which is used to illustrate the influence of deterministic factors on the bacterial community (Kraft et al., 2011), was much higher in the pit and headstream samples than in the river samples for both the whole and the rare communities (Table S6).

3.3. Co-occurrence networks of bacterial communities

Bacterial co-occurrence patterns across permafrost thawing gradients were explored using network analysis based on strong and significant correlations (Fig. 2). The number of positive correlations was predominant in all networks (Table S7). Overall, the ecological network of river samples was smaller than that of pit and headstream samples, which had twice as many nodes, edges and modules and a twice as long average path length. However, the graph density and average degree of the river network were larger, indicating tighter connection of nodes in the river network (Fig. 2; Table S7). In all networks, a substantial amount of rare taxa and few abundant taxa interacted more with themselves than with others. A module in the network is a collection of OTUs that are highly connected among themselves but have much fewer links with OTUs outside the group. The numbers of modules in the pit (10 modules) and headstream (17 modules) networks were much higher than in the river network (4 modules) (Fig. 2; Fig. S4;

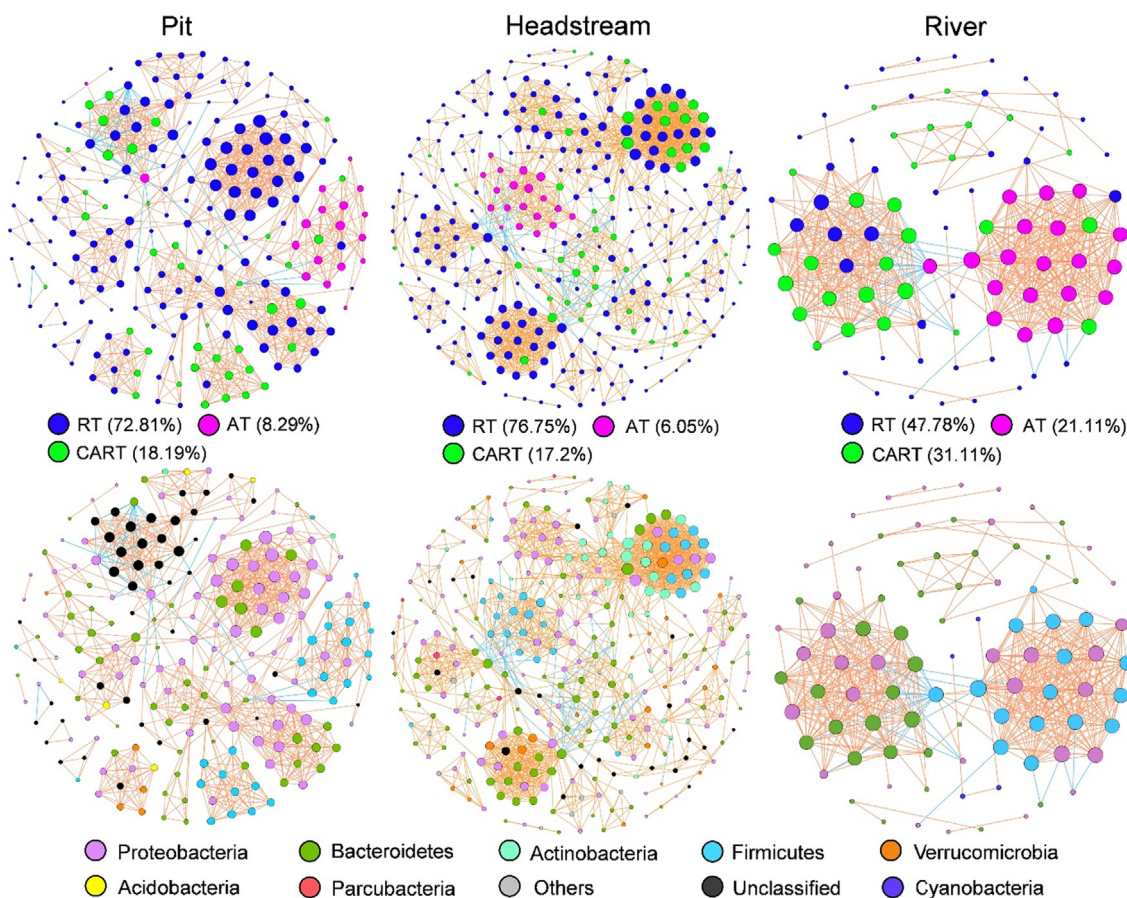


Fig. 2. The networks of co-occurring OTUs across permafrost thawing gradients from pits (left) to headstreams (middle) and to rivers (right) based on correlation analysis. A connection stands for a strong (Spearman $r > 0.6$ or $r < -0.6$) and significant ($p\text{-value} < 0.05$) correlation. For each panel, the size of each node is proportional to the number of connections (i.e. degree). The blue and orange edges indicate negative and positive interactions between two individual nodes, respectively. AT: abundant taxa, RT: rare taxa, CART: conditionally abundant and rare taxa. (For interpretation of the references to colour in this figure legend, the reader is referred to the web version of this article.)

Table S7.

The potential functions of the abundant bacterial subcommunities determined by FAPROTAX included chemoheterotrophy, aromatic compound degradation and fermentation by the abundant genera *Citrobacter* and *Acinetobacter* of *Gammaproteobacteria*. The most abundant functions of the rare bacterial subcommunities contained chemoheterotrophy, fermentation, ureolysis, phototrophy, nitrification, aerobic ammonia oxidation, aromatic compound degradation and nitrate reduction (Table S8). In addition, as much as 76.3% of all OTUs could not be assigned to any group, indicating a so far insufficient understanding of bacterial functions in permafrost environments.

3.4. DOM composition across permafrost thawing gradients

Six components of the PARAFAC model (Figs. S5 and S6) were compared with those published in the OpenFluor database (Murphy et al., 2014). The components C1 and C2 (Ex/Em = 240/412 nm) represented microbial humic-like DOM and terrestrial humic-like fluorophores, respectively (Huang et al., 2013; Shutova et al., 2014). The component C6 (335(250)/428 nm) is also linked to humic-like or fulvic-like fluorophores (Zhou et al., 2017). The components C3 (< 230(290)/356 nm) and C5 (290(250)/340 nm) were categorised as red-shifted tryptophan-like and tryptophan-like fluorophores, respectively (Stedmon and Markager, 2005). C4 (< 230(275)/308 nm) included tyrosine-like (Peak B) fluorophores (Murphy et al., 2011). The humic-like component C1 (47.3 ± 8.9%) was predominant among the permafrost thawing gradients, followed by C2 (18.8 ± 5.1%), C3

(11.3 ± 7.8%), C4 (11.1 ± 6.9%), C5 (6.1 ± 2.7%) and C6 (5.4 ± 3.3%). All components differed significantly over site and month (two-way ANOVA, $p < 0.05$), and the effect of site was much higher than that of month (Table S9; Fig. S7). The mean value of all components decreased steeply from pits to headstreams and to rivers in all months (Fig. S7).

Thousands of molecular formulae were detected via FT-ICR-MS in 14 samples and could be categorised according to their O/C versus H/C ratios (Table S10). All samples contained the highest relative proportions of formulae representing lignins (56.9 ± 9.7%), followed by tannins (13.7 ± 10.3%) and condensed aromatics (7.8 ± 2.1%), and relatively lower proportions of proteins (6.8 ± 2.5%), lipids (5.5 ± 1.2%), carbohydrates (4.4 ± 0.7%) and unsaturated hydrocarbons (4.0 ± 1.6%). This molecular composition displayed typical soil- and plant-derived origins (Spencer et al., 2015). In addition, the relative proportions of formulae containing CHO (35.4 ± 2.9%), CHON (26.6 ± 5.3%), CHOS (23.0 ± 5.9%) and CHONS (15.0 ± 3.3%) were comparatively balanced.

3.5. Linkages between bacterial communities and DOM composition

Mantel tests showed that the changes in the composition of the whole and the rare communities were significantly related to differences in the measured physicochemical parameters (Table S11). Specifically, TDS, pH and the concentrations of DOC, TDN, TDP and NO_3^- were significant factors (Table S11). In contrast, only elevation, TDS and DOC were significant factors for the composition changes of the

Table 1

Mantel tests between pairwise bacterial dissimilarities, standard effect size determined by null model analysis and DOM optical and molecular composition (Euclidean distances) for the whole, the abundant and rare bacterial communities.

	All	Abundant	Rare
<i>Optical composition (number of samples = 54)</i>			
Bray-Curtis dissimilarity	0.57 (< 0.001)	0.21 (0.012)	0.52 (< 0.001)
Jaccard dissimilarity	0.52 (< 0.001)	–	0.52 (< 0.001)
Standard effect size (SES)	0.45 (< 0.001)	– 0.16 (0.997)	0.45 (< 0.001)
<i>Molecular composition (number of samples = 14)</i>			
Bray-Curtis dissimilarity	0.57 (0.002)	0.30 (0.07)	0.51 (< 0.001)
Jaccard dissimilarity	0.53 (0.007)	–	0.52 (0.004)
Standard effect size (SES)	0.53 (0.003)	– 0.24 (0.94)	0.49 (0.013)

The number in the bracket indicates the significance tested based on 999 permutations. Note that abundant OTUs were persistent in all samples and that the incidence-based Jaccard dissimilarity cannot be calculated. Optical composition indicates six fluorescence components; Molecular composition indicates all assigned molecular peaks.

abundant subcommunities. Mantel tests further revealed that the differences in DOM optical and molecular composition were significantly correlated with the changes in the whole and rare communities across permafrost thawing gradients (Spearman $r > 0.45$, $p < 0.01$; Table 1). In contrast, only the differences in DOM fluorescence composition were related to the changes in the abundant communities (Spearman $r = 0.21$, $p < 0.05$; Table 1), and other correlations were not significant ($p > 0.05$; Table 1).

As for the diversity indices, multiple regression model analyses showed that the measured physicochemical parameters explained 71.9% and 75.9% of the variability of the Shannon index and the Bray-Curtis dissimilarity index for the whole bacterial community, respectively (Table S12). The most important parameters (explained variability > 10%) for the Shannon index included the concentrations of DOC (20.5%) and TDP (19.4%). For the Bray-Curtis dissimilarity index, the most important parameters were DOC (21.6%), NO_3^- (12.4%) and TDP (11.8%) concentrations. In addition, the determinant coefficients of the multiple regression models were higher in the rare subcommunities than in the abundant subcommunities (Table S12). The concentration of DOC together with the intensities of all fluorescence components decreased steeply from pits to headstreams and to rivers, as well as from May to July and to September (Table S1; Fig. S7), and the diversity indices of the whole and the rare communities decreased with decreasing DOC concentrations and declining intensities of all fluorescence components (Fig. S8; Table S13). However, a much weaker correlation was observed between the Bray-Curtis dissimilarity indices of the abundant communities and DOC concentrations, and no obvious relationship occurred between the alpha-diversities of the abundant communities and DOC concentrations or the intensities of fluorescence components (Fig. S8).

Bacterial alpha- and beta-diversities of the abundant and rare subcommunities showed distinct correlations with the relative intensities of molecular formulae as well (Fig. 3). The molecular formulae selected (Spearman $r \geq 0.4$) were mostly categorised as lignins, tannins and condensed aromatics, which were dominant in permafrost thawing samples. The whole and the rare communities had more selected formulae than the abundant communities and stronger correlations between alpha and beta-diversity indices with molecular formulae (Fig. 3). The positive and negative correlations between the relative intensities of molecular formulae and bacterial diversity indices, including Shannon, Invsimpson and Bray-Curtis dissimilarity (Fig. 3), as well as Chao 1, Pielou's evenness and Jaccard dissimilarity (Fig. S9), distributed differently in van Krevelen diagrams. The diversity indices of the whole and rare communities were positively related to the relative intensities of tannins, condensed aromatics and more aromatic

and oxidized lignins, but negatively related to the relative intensities of proteins and sugars and less aromatic and oxidized lignins (Fig. 3; Fig. S9). In contrast, the abundant communities showed relatively irregular and opposite distribution patterns of positive and negative correlations (Fig. 3).

The correlation-based network between OTUs and assigned formulae (Fig. 4) contains 132 OTUs, 2429 molecular peaks nodes and 286,834 edges, displaying the robust co-occurrence of DOM molecular formulae containing CHO, CHON, CHOS and CHONS. Sixteen of 19 top nodes with high degree (number of connections > 20) belonged to abundant taxa (Fig. 4; Table S14) and mainly showed connections with assigned molecular peaks, including CHO and S-containing formulae (Fig. 4). These top nodes with high degree belonged to the classes of *Bacilli*, *Gammaproteobacteria*, *Sphingobacteriia* and *Alphaproteobacteria*. In contrast, the majority of selected rare taxa had much lower connections with molecular peaks and displayed correlation with CHO and CHON formulae (Fig. 4).

3.6. Changes of microbial metabolic profiles across permafrost thawing gradients

The incubated pit, headstream, and river samples displayed distinct variations in terms of relative intensities of molecular peaks before and after microbial processing (Fig. 5). Microbial assemblages from the pit sample reduced the intensity of masses with relatively lower m/z ions (< 350 m/z) and increased intensity of higher m/z ions (> 350 m/z) (Fig. 5). For the headstream and river samples, however, decreased intensity of higher m/z ions and enhanced intensity of lower m/z ions were observed after microbial degradation (Fig. 5). To further assess the metabolic roles of the microbial communities across permafrost thawing gradients, we separated the formulae into bio-degraded (compounds that showed reduced intensities or disappeared during dark incubation) and bio-produced (compounds that showed increased intensities or were absent in the pre-incubation sample and were produced during the course of the incubation) groups. According to bio-degraded and bio-produced formulae in van Krevelen diagrams, microbial assemblages from the pit sample mainly relied on tannins, condensed aromatics and more aromatic and oxidised lignins, which highly overlapped with formulae showing positive correlations with the diversity indices of the whole and rare bacterial communities (Fig. 5; Table S15). Meanwhile, lipids, unsaturated hydrocarbons, proteins and a large part of lignins were produced after microbial processes (Fig. 5; Table S15). Decreasing metabolic diversities of microbial assemblages in the headstream and river samples were observed, and this decrease mainly manifested itself as less utilised tannins and condensed aromatics and less generated proteins and lipids (Fig. 5). Especially for the river sample, microbial metabolic formulae mainly concentrated on lignins and displayed high overlap between bio-degraded and bio-produced formulae, reflecting relatively narrow metabolic capabilities.

4. Discussion

4.1. Mechanisms underlying the assemblages of abundant and rare subcommunities

Our results showed that the rare subcommunities overwhelmingly contributed to the changes of the bacterial communities along the permafrost thawing gradients. This is supported by overall concurrent changes of the richness, evenness and dissimilarity of the whole and rare communities, whereas distinct biodiversity patterns of the abundant subcommunities occurred along the permafrost thawing gradients (Table S3; Fig S1). The significantly higher dissimilarities of the rare subcommunities than of the abundant subcommunities (Fig. 2; Table S5) also indicated a highly dynamic alteration of rare taxa and a stable persistence of a few abundant taxa characterised as cold tolerant (such as *Exiguobacterium*). In addition, the percentage contribution of rare

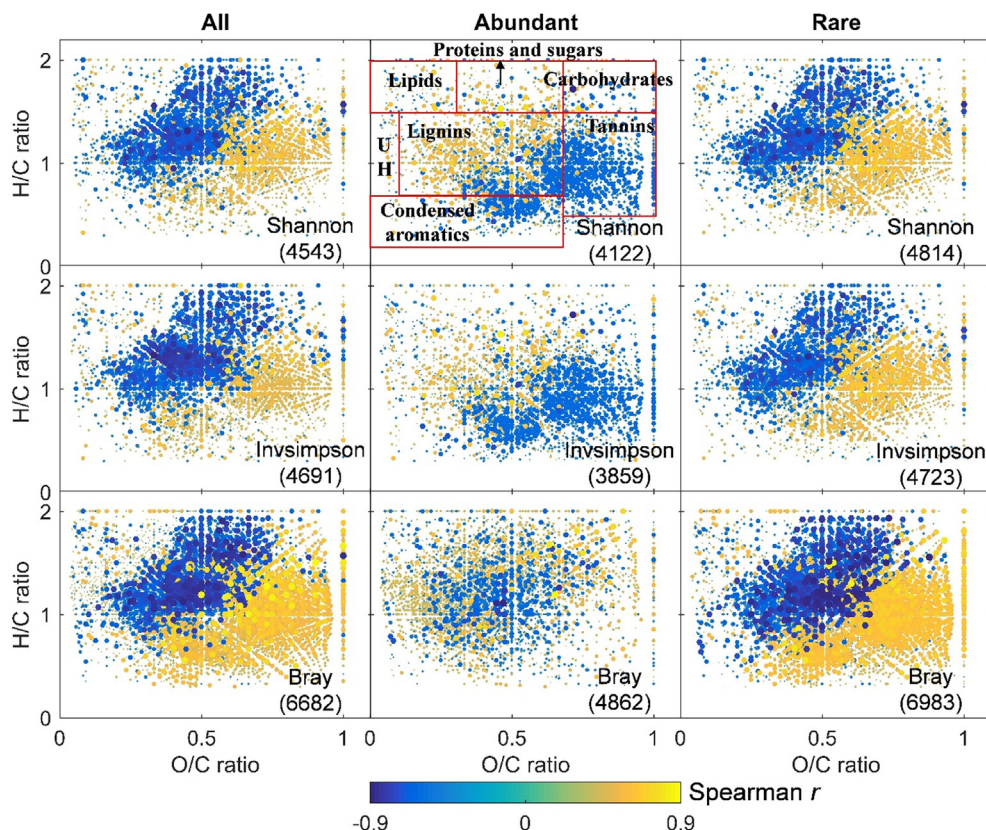


Fig. 3. van Krevelen diagrams show the correlations between the relative intensities of molecular formulae and bacterial diversity indices (Shannon, Invsimpson and Bray-Curtis dissimilarity) for the whole, the abundant and rare communities calculated from 14 samples across permafrost thawing gradients. UH: unsaturated hydrocarbons. Similar correlations with other diversity indices of the rare bacterial communities (Pielou's evenness, Jaccard dissimilarity and Chao 1) are shown in Fig. S9.

taxa was, evidently higher in our study than in previous reported lowland lakes, reservoirs and coastal bays (Campbell et al., 2011; Li et al., 2017; Liu et al., 2015; Mo et al., 2018), likely reflecting that permafrost-thawing environments with a permafrost soil-derived origin provide more microenvironments or microniches for rare taxa (Lynch and Neufeld, 2015).

Our null model tests further showed the major role of deterministic processes in shaping the whole and rare bacterial communities. In contrast, the stochastic processes were more important for the abundant subcommunities (Table S6). Among ecological mechanisms, selection is deterministic and drift is stochastic, and speciation and dispersal could contribute to both (Ren et al., 2017; Zhou et al., 2014). Considering the fluidic feature of permafrost thawing gradients and the time span of sampling (4 month), dispersal and speciation might not be major limiting factors. Therefore, environmental selection imposed by the abiotic environment (environmental filtering) and biotic interactions (Dumbrell et al., 2010; Hu et al., 2015) mainly contributed to the changes of the whole and rare communities which almost all derived from species replacement (Table S5). The dynamics of the abundant communities, mainly ascribed to species nestedness, was driven by ecological drift. Moreover, all indicator OTUs were composed of rare and conditionally abundant and rare taxa (Table S4), further suggesting higher sensitivity of the rare taxa to environmental changes in permafrost-thawing environments. This might be due to rare taxa serving as an active microbial seed bank with a pool of ecological potential (Cáceres and Legendre, 2009; Lynch and Neufeld, 2015).

Network analysis offers an integrated understanding of bacterial community assembly rules reflecting ecological processes, such as cooperation, competition and niche partitioning (Jiang et al., 2017). Predominant positive connections in all networks suggest that cooperation played a major role in these interactions. Moreover, a substantial number of rare taxa and a few abundant taxa interacted more with themselves than with other taxa and formed modular structures with themselves (Fig. 2), which further suggested the different

functional roles and niche partitioning of abundant and rare subcommunities (Eiler et al., 2012). Furthermore, the potential functions of bacterial communities determined by FAPROTAX revealed that rare taxa contributed not only to the functions of carbon processing, including aromatic compound degradation and fermentation, as in the case of abundant taxa, but also the functions related to nutrient cycling, such as nitrification, nitrate reduction and aerobic ammonia oxidation (Table S8). This greater taxonomic and functional diversity emphasises the crucial role of “rare biosphere” in regulating biogeochemical cycles and in maintaining ecosystem functions in permafrost thawing environments.

4.2. Responses of abundant and rare communities to DOM quantity and composition

Our results showed that the DOC concentration, together with the TDP and NO_3^- concentration, explained the largest proportion of the variability in the bacterial diversity indices (Table S12). Thus higher DOC concentration, implying a larger amount of dissolved organic carbon and energy supplies, can sustain a bacterial community with higher diversity (Lennon and Pfaff, 2005; Li et al., 2012). This might explain the significant positive correlations between richness, evenness, dissimilarities of the whole (rare) bacterial community and DOC concentrations, humic-like, protein-like components of DOM along permafrost thawing gradients (Fig. S8; Table S13). The responses of diversities of the ecological drift-driven abundant subcommunities to DOC concentration and fluorescence components were much weaker and not evident (Fig. S8), as was expected. In addition to the overall quantity, the bioavailability of DOM also influences bacterial activity and community (Coelen et al., 2011; Roehm et al., 2009; Vonk et al., 2013, 2015). Previous studies conducted in the Tibetan Plateau and in Arctic regions found that the biodegradability of permafrost-derived DOM (BDOM) decreased from headwater streams to large river systems (Abbott et al., 2014; Mann et al., 2012; Wang et al., 2018a), the

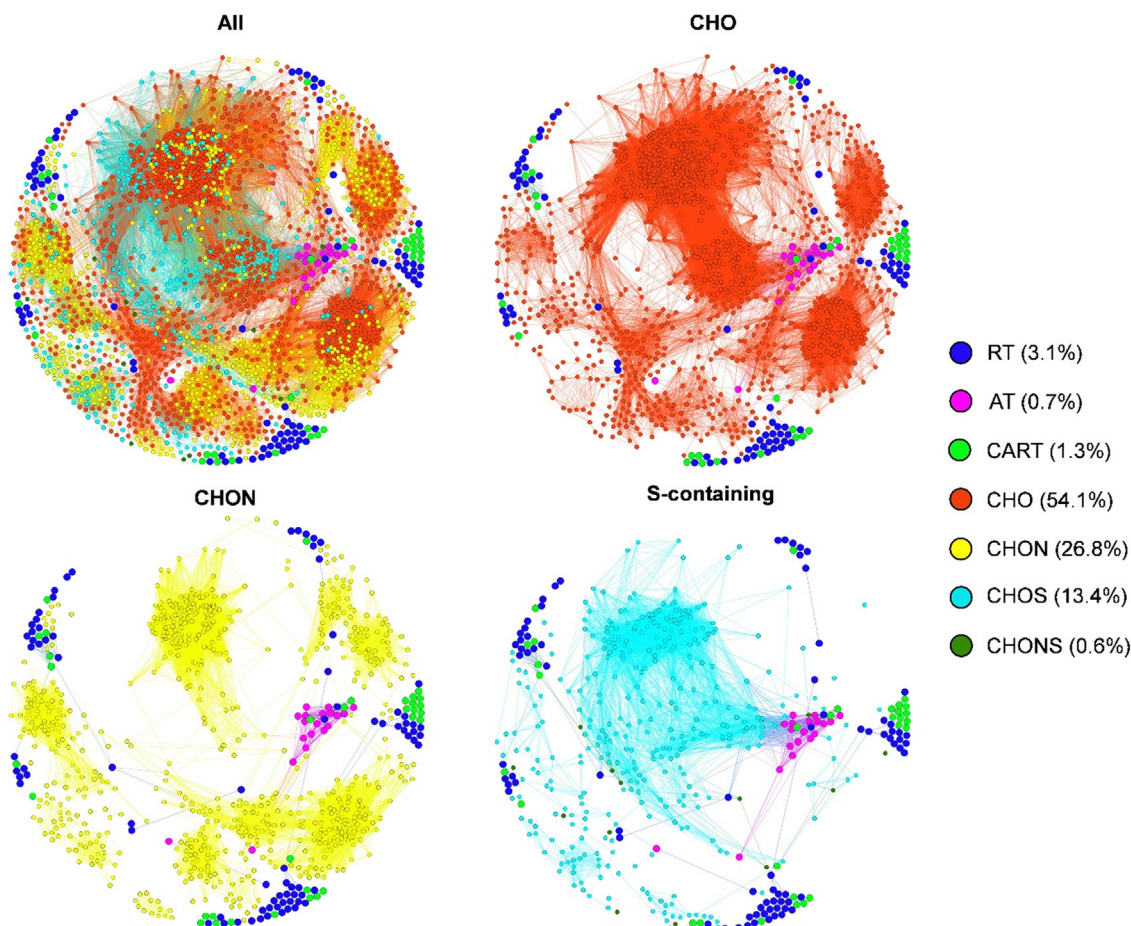


Fig. 4. Network layout showing the correlation between OTUs and assigned all, CHO, CHON and S-containing (CHOS and CHONS) formulae. A connection stands for a strong (Spearman $r > 0.8$ or $r < -0.8$) and significant ($p\text{-value} < 0.01$) correlation. The blue and orange edges indicate negative and positive interactions between two individual nodes, respectively. AT: abundant taxa, RT: rare taxa, CART: conditionally abundant and rare taxa. (For interpretation of the references to colour in this figure legend, the reader is referred to the web version of this article.)

strongest loss of BDOM occurring in headstreams (Frey et al., 2016; Liu et al., 2018; Mann et al., 2015; Spencer et al., 2015). Increasing supply of bioavailable DOM can sustain higher bacterial diversity (Landa et al., 2013); therefore, higher bioavailability of DOM in pits and headstreams also contributed to the higher diversity of the whole (rare) bacterial community in pits and headstreams than in rivers.

Our results further revealed that not only the conventional physicochemical parameters, such as TDS, pH and the concentration of DOC, TDN, TDP and NO_3^- , but also DOM composition seem to play a significant role in shaping bacterial community composition also in permafrost thawing environments (Table S11; Table 1). The heterogeneity of DOM composition, encompassing the changes of abundance and bioavailability of carbon and other resources (Kellerman et al., 2015; Song et al., 2019; Vonk et al., 2015), has previously been considered to be a strong selective force influencing aquatic microbial diversity and community structure (Bana et al., 2014; Landa et al., 2015; Muscarella et al., 2019; Ruiz-Gonzalez et al., 2015; Song et al., 2019; Underwood et al., 2019). The significant relationships between fluorescent and molecular composition of DOM with SES values, as well as with incidence-based and abundance-weighted dissimilarities (Table 1), confirmed that DOM composition acted as an environmental factor selecting the bacterial communities in permafrost thawing environments, most pronouncedly for the rare subcommunities. The stronger relationship between DOM heterogeneity and the rare subcommunities than with the abundant subcommunities further indicates that predominant rare taxa mostly serve as resource specialists with unique resource preferences among the bacterial

communities, as has previously been reported (Muscarella et al., 2019). Based on this, the heterogeneity of DOM can alter rare bacterial subcommunities via offering consumers more unique resource niches to partition. Abundant subcommunities may, however, perform as generalists being capable of consuming and metabolising numerous organic molecules (Egli, 2010; Muscarella et al., 2019). This was supported by a larger amount of connections of abundant taxa (OTUs belonging to the genera *Exiguobacterium*, *Acinetobacter* and *Citrobacter*) with assigned DOM formulae (CHO, CHON, CHONS) than that of rare taxa (OTUs belonging to the genera *Pedobacter*, *Brevundimonas* and *Chryseobacterium*) (Fig. 4; Table S14).

4.3. Linking the microbial metabolism of DOM with biodiversity patterns

A mutual linkage exists between the bacterial community and DOM composition (Logue et al., 2016; Muscarella et al., 2019), that is, not only resources act as environmental factors shaping bacterial communities, also bacteria play crucial roles in the transformation of DOM. Separated correlations of all and rare bacterial diversity indices with thousands of assigned formulae were observed at molecular level (Fig. 3), likely indicating the occurrence of specific metabolic niches for microbial utilisation (Hur et al., 2011; Muscarella et al., 2019; Zhou et al., 2019). This was confirmed by bio-incubation experiments showing that molecular formulae displaying positive correlations with bacterial diversities were classified as bio-degraded (Fig. 5). The finding that microbial assemblages collected from thermokarst pits and downstream rivers mainly relied on more aromatic-like compounds,

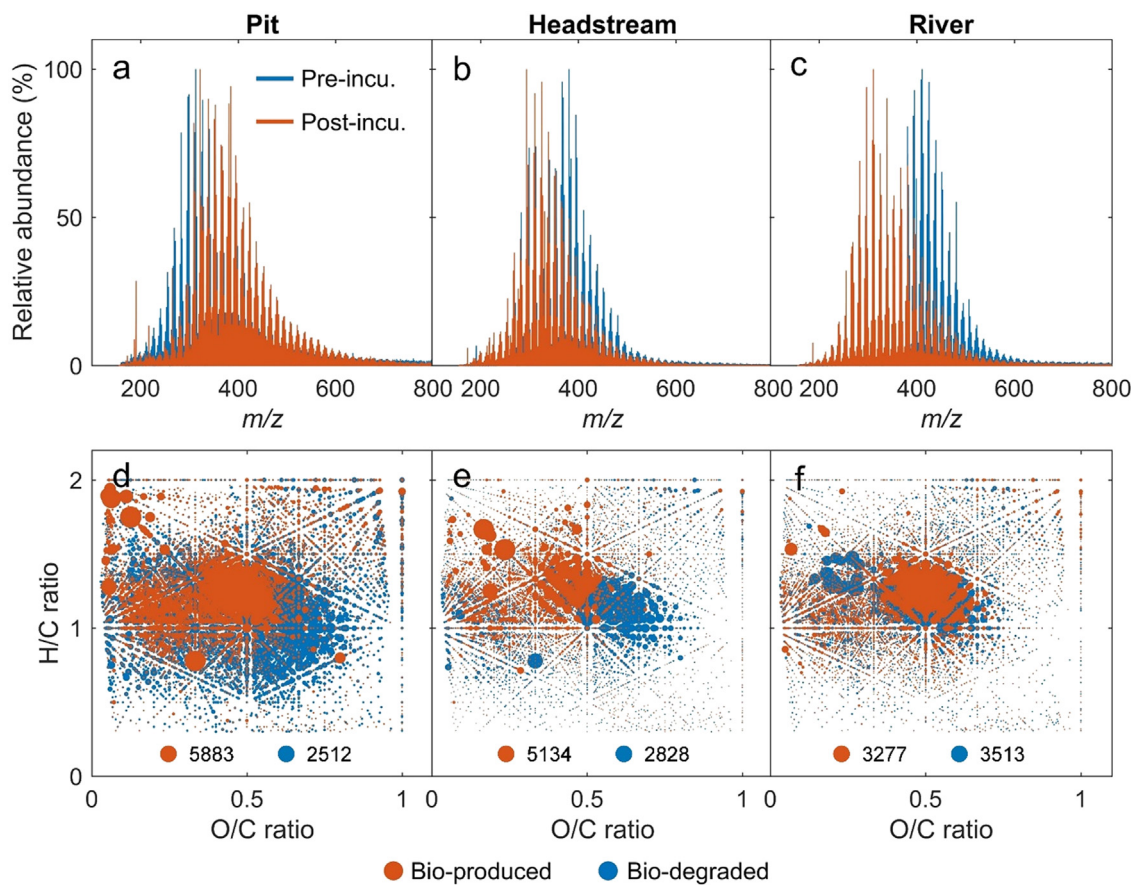


Fig. 5. Variations in DOM molecular composition of the pit (a, d), headstream (b, e) and river (c, f) sample via bio-incubation experiments. Formulae in van Krevelen diagrams were categorised as Bio-degraded by microbes (blue colour) and Bio-produced by microbes (red colour). The size of the symbol is proportional to the change in relative intensity. (For interpretation of the references to colour in this figure legend, the reader is referred to the web version of this article.)

including tannins, condensed aromatics and more oxidised lignins rather than aliphatic-like DOM expected to be more labile, is quite different from results acquired from ocean (Ogawa et al., 2001), lake (Perez and Sommaruga, 2006) and river (Melo et al., 2019) ecosystems. However, a previous study conducted in permafrost thawing environments of the Arctic region also demonstrated microbial consumption of aromatic-like DOC (Ward et al., 2017) (Fig. S10a), reflecting that native microbes exposed to aromatic-like compounds-enriched environments are capable of degrading these kinds of materials. In addition, photo degradation of DOM can convert larger, more aromatic, more oxidised DOM into smaller, more aliphatic, less oxidised DOM (Cory et al., 2013, 2014; Ward and Cory, 2016) (Fig. S10b). Thus, photochemical alteration of DOM may inhibit microbial activity and to some degree account for decreasing bacterial diversity with increasing photoproduced more aliphatic and less oxidised DOM (Ward et al., 2017).

Our results further revealed that decreasing bacterial diversities concurred with decreasing metabolic diversities along permafrost thawing gradients. This was supported by bio-incubation experiments showing shifts in microbial metabolic profiles, that is, reduced utilisation of tannins, condensed aromatics and more aromatic and oxidised lignins, as well as reduced production of lipids and proteins from the pit sample to the river sample (Fig. 5). Furthermore, as the modularity in network analysis can shed light on the collections of nodes performing different functions (Xue et al., 2018), much less modules in the network of river samples than in pit and headstream samples suggested reduced functional diversity of bacterial community as well. Actually, microbial communities contain a large quantity of species and exhibit complex interactions of microbes, and they often show functional redundancy (Ren et al., 2017; Wilhelm et al., 2013; Zhang et al., 2019). The

congruent decreases of bacterial diversity and corresponding metabolic diversity may be because DOM in the permafrost thawing environments was predominantly composed of materials of terrestrial origin (Table S10) and provides large amounts of micro niches for rare taxa that were highly sensitive to environmental changes. This permafrost thawing environment distinguishes itself from other aquatic ecosystems that provide relatively complex and substitutable DOM resources of autochthonous, allochthonous and anthropogenic origins for microbial utilisation (Muscarella et al., 2019; Song et al., 2019).

Increasing thaw depth in consequence of global warming can lead to the release of ancient organic carbon with greater amounts of old, aliphatic DOM, such as protein and carbohydrate, from permafrost to downstream waters (Mann et al., 2015; Schuur et al., 2009; Ward and Cory, 2015), and this is also pronounced in the Qinghai-Tibetan Plateau (Wang et al., 2018b). As a large part of bacteria rely on aromatic-like compounds, this change in the source of permafrost DOM, implying alteration of DOM bioavailability and photolability, may influence both the diversity and functioning of the bacterial communities in the permafrost thawing environment. Moreover, the effects of DOM quantity and composition on bacterial diversities and metabolic activities may be different among sites along permafrost thawing gradients, which should be further considered. These changes may ultimately alter the permafrost carbon climate feedback by affecting bacterial degradation and mineralisation in permafrost thawing environments (Lapierre et al., 2013; Mackelprang et al., 2011; Vonk et al., 2013).

5. Conclusion

Our study using high-throughput sequencing and ultrahigh-

resolution mass spectrometry combined with laboratory bio-incubation experiments revealed a significant influence of DOM quantity and composition on decreasing diversities of the rare bacterial sub-communities along permafrost thawing gradients. Moreover, more aromatic-like DOM such as tannins, more oxidised lignins and condensed aromatics, displaying positive correlations with rare bacterial diversities, were classified as bio-degraded molecules. Decreasing bacterial diversities also concurred with reduced metabolic diversities in terms of DOM consumption and production along permafrost thawing gradients. The abundant subcommunities were, however, mainly determined by ecological drift-driven stochastic processes and showed weak associations with DOM composition. These different response mechanisms of abundant and rare subcommunity diversities to the variability of permafrost DOM provide a new perspective for understanding the interactions between microbes and DOM, which plays a central role in the global carbon cycles.

Acknowledgments

This work was supported by the National Natural Science Foundation of China (grants 41621002, 41790423 and 41807362), the Provincial Natural Science Foundation of Jiangsu in China (BK20181104), the Key Research Program of Frontier Sciences, Chinese Academy of Sciences (QYZDB-SSW-DQC016) and NIGLAS Foundation (NIGLAS2017GH03 and NIGLAS2017QD08). Erik Jeppesen was supported by the WATEC (Centre for Water Technology, AU). We would like to express our deep thanks to Anne Mette Poulsen from Aarhus University for editorial assistance. We are grateful to the editor and the anonymous reviewers for their useful comments on this manuscript.

Declaration of Competing Interest

The authors declare that they have no conflict of interest.

Appendix A. Supplementary material

Supplementary data to this article can be found online at <https://doi.org/10.1016/j.envint.2019.105330>.

References

- Abbott, B.W., Larouche, J.R., Jones, J.B., Bowden, W.B., Balser, A.W., 2014. Elevated dissolved organic carbon biodegradability from thawing and collapsing permafrost. *J. Geophys. Res.: Biogeo.* 119, 2049–2063. <https://doi.org/10.1002/2014jg002678>.
- Anderson, M.J., Crist, T.O., Chase, J.M., Vellend, M., Inouye, B.D., Freestone, A.L., Sanders, N.J., Cornell, H.V., Comita, L.S., Davies, K.F., Harrison, S.P., Kraft, N.J., Stegen, J.C., Swenson, N.G., 2011. Navigating the multiple meanings of beta diversity: a roadmap for the practicing ecologist. *Ecol. Lett.* 14, 19–28. <https://doi.org/10.1111/j.1461-0248.2010.01552.x>.
- Bana, Z., Ayo, B., Marrase, C., Gasol, J.M., Iribarri, J., 2014. Changes in bacterial metabolism as a response to dissolved organic matter modification during protozoan grazing in coastal Cantabrian and Mediterranean waters. *Environ. Microbiol.* 16, 498–511. <https://doi.org/10.1111/1462-2920.12274>.
- Baselga, A., 2013. Separating the two components of abundance-based dissimilarity: balanced changes in abundance vs. abundance gradients. *Methods Ecol. Evol.* 4, 552–557. <https://doi.org/10.1111/2041-210X.12029>.
- Benjamini, Y., Hochberg, Y., 1995. Controlling the false discovery rate - a practical and powerful approach to multiple testing. *J. R. Stat. Soc. B* 57, 289–300. <https://doi.org/10.1111/j.2517-6161.1995.tb02031.x>.
- Bockheim, J.G., Munroe, J.S., 2014. Organic carbon pools and genesis of alpine soils with permafrost: a review. *Arct. Antarct. Alp. Res.* 46, 987–1006. <https://doi.org/10.1657/1938-4246-46.4.987>.
- Cáceres, M.D., Legendre, P., 2009. Associations between species and groups of sites: Indices and statistical inference. *Ecology* 90, 3566–3574. <https://doi.org/10.1890/08-1823.1>.
- Campbell, B.J., Yu, L., Heidelberg, J.F., Kirchman, D.L., 2011. Activity of abundant and rare bacteria in a coastal ocean. *Proc. Nat. Acad. Sci. USA* 108, 12776–12781. <https://doi.org/10.1073/pnas.1101405108>.
- Chen, L., Liu, L., Mao, C., Qin, S., Wang, J., Liu, F., Blagodatsky, S., Yang, G., Zhang, Q., Zhang, D., Yu, J., Yang, Y., 2018. Nitrogen availability regulates topsoil carbon dynamics after permafrost thaw by altering microbial metabolic efficiency. *Nat. Commun.* 9, 3951. <https://doi.org/10.1038/s41467-018-06232-y>.
- Chen, M., Li, C., Zeng, C., Zhang, F., Raymond, P.A., Hur, J., 2019. Immobilization of relic anthropogenic dissolved organic matter from alpine rivers in the Himalayan-Tibetan Plateau in winter. *Water Res.* 160, 97–106. <https://doi.org/10.1016/j.watres.2019.05.052>.
- Clarke, K.R., 1993. Non-parametric multivariate analyses of changes in community structure. *Aust. J. Ecol.* 18, 117–143. <https://doi.org/10.1111/j.1442-9993.1993.tb00438.x>.
- Coolen, M.J., van de Giessen, J., Zhu, E.Y., Wuchter, C., 2011. Bioavailability of soil organic matter and microbial community dynamics upon permafrost thaw. *Environ. Microbiol.* 13, 2299–2314. <https://doi.org/10.1111/j.1462-2920.2011.02489.x>.
- Cory, R.M., Crump, B.C., Dobkowski, J.A., Kling, G.W., 2013. Surface exposure to sunlight stimulates CO₂ release from permafrost soil carbon in the Arctic. *Proc. Nat. Acad. Sci. USA* 110, 3429–3434. <https://doi.org/10.1073/pnas.1214104110>.
- Cory, R.M., Ward, C.P., Crump, B.C., Kling, G.W., 2014. Carbon cycle. Sunlight controls water column processing of carbon in arctic fresh waters. *Science* 345, 925–928. <https://doi.org/10.1126/science.1253119>.
- Cottenie, K., 2005. Integrating environmental and spatial processes in ecological community dynamics. *Ecol. Lett.* 8, 1175–1182. <https://doi.org/10.1111/j.1461-0248.2005.00820.x>.
- Crevecoeur, S., Vincent, W.F., Comte, J.r.m., Lovejoy, C., 2015. Bacterial community structure across environmental gradients in permafrost thaw ponds: methanotrophic ecosystems. *Front. Microbiol.* 6, 192. <https://doi.org/10.3389/fmicb.2015.00192>.
- Drake, T.W., Wickland, K.P., Spencer, R.G., McKnight, D.M., Striegl, R.G., 2015. Ancient low-molecular-weight organic acids in permafrost fuel rapid carbon dioxide production upon thaw. *Proc. Nat. Acad. Sci. USA* 112, 13946–13951. <https://doi.org/10.1073/pnas.1511705112>.
- Dumbrell, A.J., Nelson, M., Helgason, T., Dytham, C., Fitter, A.H., 2010. Relative roles of niche and neutral processes in structuring a soil microbial community. *ISME J.* 4, 337–345. <https://doi.org/10.1038/ismej.2009.122>.
- Edgar, R.C., 2010. Search and clustering orders of magnitude faster than BLAST. *Bioinformatics* 26, 2460–2461. <https://doi.org/10.1093/bioinformatics/btp461>.
- Egli, T., 2010. How to live at very low substrate concentration. *Water Res.* 44, 4826–4837. <https://doi.org/10.1016/j.watres.2010.07.023>.
- Eiler, A., Heinrich, F., Bertilsson, S., 2012. Coherent dynamics and association networks among lake bacterioplankton taxa. *ISME J.* 6, 330–342. <https://doi.org/10.1038/ismej.2011.113>.
- Erdős, P., Rényi, A., 1960. On the evolution of random graphs. *Publ. Math. Inst. Hung. Acad. Sci.* 5, 17–60.
- Frey, K., Sobczak, W., Mann, P., Holmes, R., 2016. Optical properties and bioavailability of dissolved organic matter along a flow-path continuum from soil pore waters to the Kolyma River mainstem, East Siberia. *Biogeosci.* 13, 2279–2290. <https://doi.org/10.5194/bg-13-2279-2016>.
- Heimann, M., Reichstein, M., 2008. Terrestrial ecosystem carbon dynamics and climate feedbacks. *Nature* 451, 289–292. <https://doi.org/10.1038/nature06591>.
- Hu, W., Zhang, Q., Tian, T., Li, D., Cheng, G., Mu, J., Wu, Q., Niu, F., Stegen, J.C., An, L., Feng, H., 2015. Relative Roles of deterministic and stochastic processes in driving the vertical distribution of bacterial communities in a permafrost core from the Qinghai-Tibet Plateau, China. *PLoS One* 10, e0145747. <https://doi.org/10.1371/journal.pone.0145747>.
- Huang, C.-C., Li, Y.-M., Yang, H., Sun, D.-Y., Xu, L.-J., Chen, X., 2013. Study of influencing factors to chromophoric dissolved organic matter absorption properties from fluorescence features in Taihu lake in autumn. *J. Limnol.* 72. <https://doi.org/10.4081/jlimol.2013.e26>.
- Hur, J., Lee, B.M., Shin, H.S., 2011. Microbial degradation of dissolved organic matter (DOM) and its influence on phenanthrene-DOM interactions. *Chemosphere* 85, 1360–1367. <https://doi.org/10.1016/j.chemosphere.2011.08.001>.
- Jiang, Y., Li, S., Li, R., Zhang, J., Liu, Y., Lv, L., Zhu, H., Wu, W., Li, W., 2017. Plant cultivars imprint the rhizosphere bacterial community composition and association networks. *Soil. Biol. Biochem.* 109, 145–155. <https://doi.org/10.1016/j.soilbio.2017.02.010>.
- Jousset, A., Benhield, C., Chatzinotas, A., Gallien, L., Gobet, A., Kurm, V., Kusel, K., Rillig, M.C., Rivett, D.W., Salles, J.F., van der Heijden, M.G., Youssef, N.H., Zhang, X., Wei, Z., Hol, W.H., 2017. Where less may be more: how the rare biosphere pulls ecosystems strings. *ISME J.* 11, 853–862. <https://doi.org/10.1038/ismej.2016.174>.
- Kellerman, A.M., Kothawala, D.N., Dittmar, T., Tranvik, L.J., 2015. Persistence of dissolved organic matter in lakes related to its molecular characteristics. *Nat. Geosci.* 8, 454–457. <https://doi.org/10.1038/geo2440>.
- Kothawala, D.N., Stedmon, C.A., Muller, R.A., Weyhenmeyer, G.A., Kohler, S.J., Tranvik, L.J., 2014. Controls of dissolved organic matter quality: evidence from a large-scale boreal lake survey. *Global Change Biol.* 20, 1101–1114. <https://doi.org/10.1111/gcb.12488>.
- Kraft, N.J., Comita, L.S., Chase, J.M., Sanders, N.J., Swenson, N.G., Crist, T.O., Stegen, J.C., Vellend, M., Boyle, B., Anderson, M.J., Cornell, H.V., Davies, K.F., Freestone, A.L., Inouye, B.D., Harrison, S.P., Myers, J.A., 2011. Disentangling the drivers of beta diversity along latitudinal and elevational gradients. *Science* 333, 1755–1758. <https://doi.org/10.1126/science.1208584>.
- Kramshoj, M., Albers, C.N., Svendsen, S.H., Bjorkman, M.P., Lindwall, F., Bjork, R.G., Rinnan, R., 2019. Volatile emissions from thawing permafrost soils are influenced by meltwater drainage conditions. *Global Change Biol.* 25, 1704–1716. <https://doi.org/10.1111/gcb.14582>.
- Landa, M., Blain, S., Christaki, U., Monchy, S., Obernosterer, I., 2015. Shifts in bacterial community composition associated with increased carbon cycling in a mosaic of phytoplankton blooms. *ISME J.* 10, 39–50. <https://doi.org/10.1038/ismej.2015.105>.
- Landa, M., Cottrell, M.T., Kirchman, D.L., Blain, S., Obernosterer, I., 2013. Changes in bacterial diversity in response to dissolved organic matter supply in a continuous culture experiment. *Aquat. Microb. Ecol.* 69, 157–168. <https://doi.org/10.3354/aqe0354>

- ame01632.
- Lapierre, J.F., Guillemette, F., Berggren, M., del Giorgio, P.A., 2013. Increases in terrestrially derived carbon stimulate organic carbon processing and CO₂ emissions in boreal aquatic ecosystems. *Nat. Commun.* 4, 2972. <https://doi.org/10.1038/ncomms3972>.
- Lennon, J.T., Pfaff, L.E., 2005. Source and supply of terrestrial organic matter affects aquatic microbial metabolism. *Aquat. Microb. Ecol.* 39, 107–119. <https://doi.org/10.3354/ame039107>.
- Li, D., Sharp, J.O., Saikaly, P.E., Ali, S., Alidina, M., Alarawi, M.S., Keller, S., Hoppe-Jones, C., Drewes, J.E., 2012. Dissolved organic carbon influences microbial community composition and diversity in managed aquifer recharge systems. *Appl. Environ. Microbiol.* 78, 6819–6828. <https://doi.org/10.1128/AEM.01223-12>.
- Li, H., Zeng, J., Ren, L., Wang, J., Xing, P., Wu, Q.L., 2017. Contrasting patterns of diversity of abundant and rare bacterioplankton in freshwater lakes along an elevation gradient. *Limnol. Oceanogr.* 62, 1570–1585. <https://doi.org/10.1002/lno.10518>.
- Liu, F., Chen, L., Zhang, B., Wang, G., Qin, S., Yang, Y., 2018. Ultraviolet radiation rather than inorganic nitrogen increases dissolved organic carbon biodegradability in a typical thermo-erosion gully on the Tibetan Plateau. *Sci. Total Environ.* 627, 1276–1284. <https://doi.org/10.1016/j.scitotenv.2018.01.257>.
- Liu, L., Yang, J., Yu, Z., Wilkinson, D.M., 2015. The biogeography of abundant and rare bacterioplankton in the lakes and reservoirs of China. *ISME J.* 9, 2068–2077. <https://doi.org/10.1038/ismej.2015.29>.
- Logares, R., Audic, S., Bass, D., Bittner, L., Boutte, C., Christen, R., Claverie, J.M., Decelle, J., Dolan, J.R., Dunthorn, M., Edvardsen, B., Gobet, A., Kooistra, W.H., Mahe, F., Not, F., Ogata, H., Pawłowski, J., Pernice, M.C., Romac, S., Shalchian-Tabrizi, K., Simon, N., Stoeck, T., Santini, S., Siano, R., Wincker, P., Zingone, A., Richards, T.A., de Vargas, C., Massana, R., 2014. Patterns of rare and abundant marine microbial eukaryotes. *Curr. Biol.* 24, 813–821. <https://doi.org/10.1016/j.cub.2014.02.050>.
- Logue, J.B., Stedmon, C.A., Kellerman, A.M., Nielsen, N.J., Andersson, A.F., Laudon, H., Lindstrom, E.S., Kritzberg, E.S., 2016. Experimental insights into the importance of aquatic bacterial community composition to the degradation of dissolved organic matter. *ISME J.* 10, 533–545. <https://doi.org/10.1038/ismej.2015.131>.
- Louca, S., Jacques, S.M.S., Pires, A.P.F., Leal, J.S., Srivastava, D.S., Parfrey, L.W., Farjalla, V.F., Doebeli, M., 2017. High taxonomic variability despite stable functional structure across microbial communities. *Nat. Ecol. Evol.* 1, 0015. <https://doi.org/10.1038/s41559-016-0015>.
- Lynch, M.D., Neufeld, J.D., 2015. Ecology and exploration of the rare biosphere. *Nat. Rev. Microbiol.* 13, 217–229. <https://doi.org/10.1038/nrmicro3400>.
- Mackelprang, R., Waldrop, M.P., DeAngelis, K.M., David, M.M., Chavarria, K.L., Blazewicz, S.J., Rubin, E.M., Jansson, J.K., 2011. Metagenomic analysis of a permafrost microbial community reveals a rapid response to thaw. *Nature* 480, 368–371. <https://doi.org/10.1038/nature10576>.
- Mann, P.J., Davydova, A., Zimov, N., Spencer, R., Davydov, S., Bulygina, E., Zimov, S., Holmes, R., 2012. Controls on the Composition and Lability of Dissolved Organic Matter in Siberia's Kolyma River Basin. *J. Geophys. Res.: Biogeog.* 117, G01028. <https://doi.org/10.1029/2011JG001798>.
- Mann, P.J., Eglinton, T.I., McIntyre, C.P., Zimov, N., Davydova, A., Vonk, J.E., Holmes, R.M., Spencer, R.G., 2015. Utilization of ancient permafrost carbon in headwaters of Arctic fluvial networks. *Nat. Commun.* 6, 7856. <https://doi.org/10.1038/ncomms8856>.
- McCalley, C.K., Woodcroft, B.J., Hodgkins, S.B., Wehr, R.A., Kim, E.H., Mondav, R., Crill, P.M., Chanton, J.P., Rich, V.I., Tyson, G.W., Saleska, S.R., 2014. Methane dynamics regulated by microbial community response to permafrost thaw. *Nature* 514, 478–481. <https://doi.org/10.1038/nature13798>.
- Melo, M.L., Kothawala, D.N., Bertilsson, S., Amaral, J.H., Forsberg, B., Sarmento, H., 2019. Linking dissolved organic matter composition and bacterioplankton communities in an Amazon floodplain system. *Limnol. Oceanogr.* <https://doi.org/10.1002/lno.11250>.
- Mo, Y., Zhang, W., Yang, J., Lin, Y., Yu, Z., Lin, S., 2018. Biogeographic patterns of abundant and rare bacterioplankton in three subtropical bays resulting from selective and neutral processes. *ISME J.* 12, 2198–2210. <https://doi.org/10.1038/s41396-018-0153-6>.
- Mu, C., Zhang, T., Zhang, X., Li, L., Guo, H., Zhao, Q., Cao, L., Wu, Q., Cheng, G., 2016. Carbon loss and chemical changes from permafrost collapse in the northern Tibetan Plateau. *J. Geophys. Res.: Biogeog.* 121, 1781–1791. <https://doi.org/10.1002/2015JG003235>.
- Murphy, K.R., Hambly, A., Singh, S., Henderson, R.K., Baker, A., Stuetz, R., Khan, S.J., 2011. Organic matter fluorescence in municipal water recycling schemes: toward a unified PARAFAC model. *Environ. Sci. Technol.* 45, 2909–2916. <https://doi.org/10.1021/es103015e>.
- Murphy, K.R., Stedmon, C.A., Wenig, P., Bro, R., 2014. OpenFluor—an online spectral library of auto-fluorescence by organic compounds in the environment. *Anal. Methods* 6, 658–661. <https://doi.org/10.1039/c3ay41935e>.
- Muscarella, M.E., Boot, C.M., Broekeling, C.D., Lennon, J.T., 2019. Resource heterogeneity structures aquatic bacterial communities. *ISME J.* 13, 2183–2195. <https://doi.org/10.1038/s41396-019-0427-7>.
- Ogawa, H., Amagai, Y., Koike, I., Kaiser, K., Benner, R., 2001. Production of refractory dissolved organic matter by bacteria. *Science* 292, 917–920.
- Ohno, T., Parr, T.B., Gruselle, M.C.C.I., Fernandez, I.J., Sleighter, R.L., Hatcher, P.G., 2014. Molecular composition and biodegradability of soil organic matter: a case study comparing two new England forest types. *Environ. Sci. Technol.* 48, 7229–7236.
- Ordoñez, O.F., Lanzarotti, E., Kurth, D., Gorriti, M.F., Revale, S., Cortez, N., Vazquez, M.P., Farías, M.E., Turjanski, A.G., 2013. Draft genome sequence of the poly-extremophilic *Exiguobacterium* sp. strain S17, isolated from hyperarsenic lakes in the Argentinian Puna. *Genome Announc.* 1 e00480-00413.
- Pedros-Alio, C., 2012. The rare bacterial biosphere. *Annu. Rev. Mar. Sci.* 4, 449–466. <https://doi.org/10.1146/annurev-marine-120710-100948>.
- Perez, M.T., Sommaruga, R., 2006. Differential effect of algal- and soil-derived dissolved organic matter on alpine lake bacterial community composition and activity. *Limnol. Oceanogr.* 51, 2527–2537.
- Ren, L., He, D., Chen, Z., Jeppesen, E., Lauridsen, T.L., Sondergaard, M., Liu, Z., Wu, Q.L., 2017. Warming and nutrient enrichment in combination increase stochasticity and beta diversity of bacterioplankton assemblages across freshwater mesocosms. *ISME J.* 11, 613–625. <https://doi.org/10.1038/ismej.2016.159>.
- Roehm, C.L., Giesler, R., Karlsson, J., 2009. Bioavailability of terrestrial organic carbon to lake bacteria: the case of a degrading subarctic permafrost mire complex. *J. Geophys. Res.* 114, G03006. <https://doi.org/10.1029/2008jg000863>.
- Roiha, T., Peura, S., Cusson, M., Rautio, M., 2016. Allochthonous carbon is a major regulator to bacterial growth and community composition in subarctic freshwaters. *Sci. Rep.* 6, 34456. <https://doi.org/10.1038/srep34456>.
- Ruiz-Gonzalez, C., Nino-Garcia, J.P., Del Giorgio, P.A., 2015. Terrestrial origin of bacterial communities in complex boreal freshwater networks. *Ecol. Lett.* 18, 1198–1206. <https://doi.org/10.1111/ele.12499>.
- Schuur, E.A., McGuire, A.D., Schadel, C., Grosse, G., Harden, J.W., Hayes, D.J., Hugelius, G., Koven, C.D., Kuhry, P., Lawrence, D.M., Natali, S.M., Olefeldt, D., Romanovsky, V.E., Schaefer, K., Turetsky, M.R., Treat, C.C., Vonk, J.E., 2015. Climate change and the permafrost carbon feedback. *Nature* 520, 171–179. <https://doi.org/10.1038/nature14338>.
- Schuur, E.A., Vogel, J.G., Crummer, K.G., Lee, H., Sickman, J.O., Osterkamp, T.E., 2009. The effect of permafrost thaw on old carbon release and net carbon exchange from tundra. *Nature* 459, 556–559. <https://doi.org/10.1038/nature08031>.
- Shutova, Y., Baker, A., Bridgeman, J., Henderson, R.K., 2014. Spectroscopic characterisation of dissolved organic matter changes in drinking water treatment: from PARAFAC analysis to online monitoring wavelengths. *Water Res.* 54, 159–169. <https://doi.org/10.1016/j.watres.2014.01.053>.
- Singh, N.K., Raichand, R., Kaur, I., Kaur, C., Pareek, S., Mayilraj, S., 2013. *Exiguobacterium himgiriensis* sp. nov. a novel member of the genus *Exiguobacterium*, isolated from the Indian Himalayas. *Anton. Leeuw.* 103, 789–796. <https://doi.org/10.1007/s10482-012-9861-5>.
- Song, K., Shang, Y., Wen, Z., Jacinthe, P.A., Liu, G., Lyu, L., Fang, C., 2019. Characterization of CDOM in saline and freshwater lakes across China using spectroscopic analysis. *Water Res.* 150, 403–417. <https://doi.org/10.1016/j.watres.2018.12.004>.
- Spencer, R.G.M., Aiken, G.R., Wickland, K.P., Striegl, R.G., Hernes, P.J., 2008. Seasonal and spatial variability in dissolved organic matter quantity and composition from the Yukon River basin, Alaska. *Global Biogeochem. Cycles* 22, GB4002. <https://doi.org/10.1029/2008gb003231>.
- Spencer, R.G.M., Mann, P.J., Dittmar, T., Eglington, T.I., McIntyre, C., Holmes, R.M., Zimov, N., Stubbins, A., 2015. Detecting the signature of permafrost thaw in Arctic rivers. *Geophys. Res. Lett.* 42, 2830–2835. <https://doi.org/10.1002/2015GL063498>.
- Stedmon, C.A., Markager, S., 2005. Resolving the variability in dissolved organic matter fluorescence in a temperate estuary and its catchment using PARAFAC analysis. *Limnol. Oceanogr.* 50, 686–697. <https://doi.org/10.4319/lo.2005.50.2.00686>.
- Underwood, G.J.C., Michel, C., Meisterhans, G., Niemi, A., Belzile, C., Witt, M., Dumbrrell, A.J., Koch, B.P., 2019. Organic matter from Arctic sea-ice loss alters bacterial community structure and function. *Nat. Clim. Change* 9, 170–176. <https://doi.org/10.1038/s41558-018-0391-7>.
- Vonk, J.E., Mann, P.J., Davydov, S., Davydova, A., Spencer, R.G., Schade, J., Sobczak, W.V., Zimov, N., Zimov, S., Bulygina, E., 2013. High biolability of ancient permafrost carbon upon thaw. *Geophys. Res. Lett.* 40, 2689–2693.
- Vonk, J.E., Tank, S.E., Mann, P.J., Spencer, R.G.M., Treat, C.C., Striegl, R.G., Abbott, B.W., Wickland, K.P., 2015. Biodegradability of dissolved organic carbon in permafrost soils and aquatic systems: a meta-analysis. *Biogeosciences* 12, 6915–6930. <https://doi.org/10.5194/bg-12-6915-2015>.
- Wang, Y., Spencer, R.G.M., Podgorski, D.C., Kellerman, A.M., Rashid, H., Zito, P., Xiao, W., Wei, D., Yang, Y., Xu, Y., 2018a. Spatiotemporal transformation of dissolved organic matter along an alpine stream flow path on the Qinghai-Tibet Plateau: importance of source and permafrost degradation. *Biogeosciences* 15, 6637–6648. <https://doi.org/10.5194/bg-15-6637-2018>.
- Wang, Y., Xu, Y., Spencer, R.G.M., Zito, P., Kellerman, A., Podgorski, D., Xiao, W., Wei, D., Rashid, H., Yang, Y., 2018b. Selective leaching of dissolved organic matter from alpine permafrost soils on the Qinghai-Tibetan Plateau. *J. Geophys. Res.: Biogeog.* 123, 1005–1016. <https://doi.org/10.1002/2017JG004343>.
- Ward, C.P., Cory, R.M., 2015. Chemical composition of dissolved organic matter draining permafrost soils. *Geochim. Cosmochim. Acta* 167, 63–79. <https://doi.org/10.1016/j.gca.2015.07.001>.
- Ward, C.P., Cory, R.M., 2016. Complete and partial photo-oxidation of dissolved organic matter draining permafrost soils. *Environ. Sci. Technol.* 50, 3545–3553. <https://doi.org/10.1021/acs.est.5b05354>.
- Ward, C.P., Nalven, S.G., Crump, B.C., Kling, G.W., Cory, R.M., 2017. Photochemical alteration of organic carbon draining permafrost soils shifts microbial metabolic pathways and stimulates respiration. *Nat. Commun.* 8, 772. <https://doi.org/10.1038/s41467-017-00759-2>.
- Watanabe, S., Laurion, I., Chokmani, K., Pienitz, R., Vincent, W.F., 2011. Optical diversity of thaw ponds in discontinuous permafrost: A model system for water color analysis. *J. Geophys. Res.: Biogeog.* 116, G02003.
- Wilhelm, L., Singer, G., Fasching, C., Battin, T., Besemer, K., 2013. Microbial biodiversity in glacier-fed streams. *ISME J.* 7, 1651–1660. <https://doi.org/10.1038/ismej.2013.44>.
- Xue, Y., Chen, H., Yang, J.R., Liu, M., Huang, B., Yang, J., 2018. Distinct patterns and processes of abundant and rare eukaryotic plankton communities following a

- reservoir cyanobacterial bloom. ISME J. 12, 2263–2277. <https://doi.org/10.1038/s41396-018-0159-0>.
- Zhang, Z., Deng, Y., Feng, K., Cai, W., Li, S., Yin, H., Xu, M., Ning, D., Qu, Y., 2019. Deterministic assembly and diversity gradient altered the biofilm community performances of bioreactors. Environ. Sci. Technol. 53, 1315–1324. <https://doi.org/10.1021/acs.est.8b06044>.
- Zhou, J., Deng, Y., Zhang, P., Xue, K., Liang, Y., Van Nostrand, J.D., Yang, Y., He, Z., Wu, L., Stahl, D.A., Hazen, T.C., Tiedje, J.M., Arkin, A.P., 2014. Stochasticity, succession, and environmental perturbations in a fluidic ecosystem. Proc. Nat. Acad. Sci. USA 111, E836–E845. <https://doi.org/10.1073/pnas.1324044111>.
- Zhou, L., Zhou, Y., Hu, Y., Cai, J., Bai, C., Shao, K., Gao, G., Zhang, Y., Jeppesen, E., Tang, X., 2017. Hydraulic connectivity and evaporation control the water quality and sources of chromophoric dissolved organic matter in Lake Bosten in arid northwest China. Chemosphere 188, 608–617. <https://doi.org/10.1016/j.chemosphere.2017.09.006>.
- Zhou, L., Zhou, Y., Hu, Y., Cai, J., Liu, X., Bai, C., Tang, X., Zhang, Y., Jang, K.S., Spencer, R.G.M., Jeppesen, E., 2019. Microbial production and consumption of dissolved organic matter in glacial ecosystems on the Tibetan Plateau. Water Res. 160, 18–28. <https://doi.org/10.1016/j.watres.2019.05.048>.